some increase in k_r is likely to be expected in the chromophore–luminophore complex because of the additional spin–orbit coupling provided by the presence of the heavier Ru(II) metal ion in the second coordination sphere of Cr(III).[73]

Excited-State Absorption Spectrum. The long-lived excited state of the chromophore–luminophore complex is definitely localized on the luminophoric component. This notwithstanding, the ESA spectrum of the chromophore–luminophore complex is quite different from that of the free luminophore. In fact, while Cr(cyclam)$(CN)_2^+$ does not give rise to appreciable absorbance changes in the whole visible region upon excitation,[74] the ESA difference spectrum of $Ru(bpy)_2[Cr(cyclam)(CN)_2]_2^{4+}$ (Figure 3) exhibits a bleaching at 2.45 μm^{-1} and a prominent absorption which appears to peak at 1.10 μm^{-1}, both with comparable molar absorptivity changes. The assignment of these spectral features becomes straightforward upon consideration of the energy level diagram of the chromophore–luminophore complex (Figure 5), where a Ru(II) → Cr(III) IT state is expected to occur at ca. 2.5 μm^{-1}. Upon excitation of the Cr(III) center, the transition to the IT state (process f in Figure 5) is expected to be bleached and replaced by a new absorption (process g in Figure 5), red-shifted with respect to the ground-state band by an amount corresponding to the doublet energy. The energy of the bleaching compares well with the expected energy of the IT state (given the approximations involved in the estimate, see above). The shift between bleaching and absorption closely matches the doublet energy (1.37 μm^{-1}). The half-widths of the bleaching and absorption in the ESA spectrum (0.5 ± 0.1 μm^{-1}), which are related to the reorganizational energies upon ground- and excited-state electron transfer,[62] are of the same magnitude as for mixed-valence cyano-bridged polynuclear complexes.[36,65,75] The intensities of the ground- and excited-state IT bands (ϵ_{max}, ca. 1500), which reflect the degree of metal–metal electronic coupling,[62] are similar to those of IT bands of other Ru(II)–Cr(III) cyano-bridged complexes.[27,75-77] The observation of ground- and excited-state intervalence-transfer spectra, with reasonable energies, intensities, and half-widths, gives further support to the picture of these Ru(II)–Cr(III) chromophore–luminophore complexes as electronically localized species, from the standpoint of both metal oxidation states and excitation energy.

Conclusions. The electronic interaction between the molecular components in the $Ru(bpy)_2[Cr(cyclam)(CN)_2]_2^{4+}$ trinuclear complex is sufficiently weak as to allow a localized description. Nevertheless, coupling to the chromophore induces some perturbation in the luminophoric units, resulting in a narrowing of the emission band shape and an increase in radiative and radiationless rate constants. The $Ru(bpy)_2[Cr(cyclam)(CN)_2]_2^{4+}$ complex is a chromophore–luminophore complex with a number of interesting properties, among which are (i) strong visible absorption, (ii) very sharp, long-lived, and intense (for a Cr(III) system) phosphorescence, and (iii) behavior relatively independent of environment (solvent, temperature, oxygen), including good performance in water.

Acknowledgment. This work has been supported by the Ministero della Università e della Ricerca Scientifica e Tecnologica and by the Consiglio Nazionale delle Ricerche (Progetto Finalizzato Chimica Fine).

Registry No. $\{Ru(bpy)_2[Cr(cyclam)(CN)_2]_2\}(PF_6)_4$, 137467-25-5; $Ru(bpy)_2Cl_2$, 15746-57-3; *trans*-[Cr(cyclam)$(CN)_2$]Cl, 85245-74-5.

(73) Most probably, the same type of effect acts on radiationless deactivation as well (process e in Figure 5), being responsible for the shorter lifetime observed (both here and the previously studied case[27]) for the Ru(II)–Cr(III) chromophore–luminophore complex relative to the free luminophore.
(74) Indelli, M. T. Unpublished results.
(75) Vogler, A.; Osman, A. H.; Kunkely, H. *Coord. Chem. Rev.* **1985**, *64*, 15 159.
(76) Vogler, A.; Osman, A. H.; Kunkely, H. *Inorg. Chem.* **1987**, *26*, 2337.
(77) The IT intensities of the cyano-bridged Ru(II)–Cr(III) complexes are definitely smaller than those of analogous Ru(II)–Ru(III) complexes.[36,65] This may be ascribed to the smaller radial extension of Cr(III) orbitals relative to Ru(III) orbitals.

Contribution from the Department of Chemistry, College of Arts and Sciences, The University of Tokyo, Komaba, Meguro, Tokyo 153, Japan, Department of Chemistry, Faculty of Science, Tokyo Metropolitan University, Fukasawa, Setagaya, Tokyo 158, Japan, and Department of Chemistry, Faculty of Engineering, Kanagawa University, Rokkakubashi, Yokohama 221, Japan

^{13}C CP-MAS, ^{13}C, and ^1H NMR Spectroscopic Study of Mixed-Valence 1,1″-Biruthenocenium Salts

Masanobu Watanabe,*[1a] Toschitake Iwamoto,[1a] Satoshi Kawata,[1b] Atsushi Kubo,[1b] Hirotoshi Sano,[1b] and Izumi Motoyama[1c]

Received January 25, 1991

1,1″-Biruthenocene (**1**) reacts with FeX_3 salts in HX–NH_4PF_6 (X = Br, Cl) solution and with I_2, giving diamagnetic $[RcRcX]^+PF_6^-$ (**2**, X = Br; **3**, X = Cl) and $[RcRcI]^+I_3^-$ (**4**) salts, respectively. These salts are formulated as mixed-valence biruthenocenium salts $[Ru^{II}Cp(C_5H_4)(C_5H_4)CpRu^{IV}X]^+Y^-$ (X = Cl, Br, I; Y = PF_6, I_3) in the solid state on the basis of ^{13}C CP-MAS NMR spectroscopy. A rapid intramolecular electron transfer between Ru^{II} and Ru^{IV} has been observed accompanied with exchange of the X atom in organic solvent at room temperature: $[Ru^{II}Cp(C_5H_4)(C_5H_4)CpRu^{IV}X]^+ \rightleftharpoons [XRu^{IV}Cp(C_5H_4)(C_5H_4)CpRu^{II}]^+$. The electron-transfer rate increases in the order of **4** < **2** < **3** on the basis of ^{13}C and ^1H NMR spectroscopies. Upon decrease of temperature, the rate decreases, and finally, the salts contain trapped-valence states: $[Ru^{II}Cp(C_5H_4)(C_5H_4)CpRu^{IV}X]^+Y^-$.

Introduction

Trapped- and averaged-valence states have been observed for a large number of mixed-valence binuclear ferrocene derivatives.[2-4] The results of ^{57}Fe Mössbauer spectroscopy and other physicochemical measurements of the salts show that some of the monocationic salts are in either an averaged- or a trapped-valence state independent of temperature, while others are in a temperature-dependent trapped- to averaged-valence state in a pertinent temperature range. Few studies of the chemistry of 1,1″-biruthenocene and related species, however, have been reported, probably because of the low yield of biruthenocene $[RuCp(C_5H_4)(C_5H_4)CpRu]$ (abbreviated as RcRc, **1**) (Chart I).[5,6] We prepared **1** in high yield by a radical coupling of ruthenocene (RcH) in concentrated sulfuric acid at 80 °C. Mixed-valence 1,1″-biruthenocenium

(1) (a) The University of Tokyo. (b) Tokyo Metropolitan University. (c) Kanagawa University.
(2) Morrison, W. H., Jr.; Hendrickson, D. N. *Inorg. Chem.* **1975**, *14*, 2331. Kaufman, F.; Cowan, D. O. *J. Am. Chem. Soc.* **1970**, *92*, 6198.
(3) Dong, T. Y.; Hendrickson, D. N.; Iwai, K.; Cohn, M. J.; Geib, S. J.; Rheingold, A. L.; Sano, H.; Motoyama, I.; Nakashima, S. *J. Am. Chem. Soc.* **1985**, *107*, 7996.
(4) Kambara, T.; Hendrickson, D. N.; Dong, T. Y.; Cohn, M. J.; *J. Chem. Phys.* **1987**, *86*, 2362. Nakashima, S.; Sano, H. *Bull. Chem. Soc. Jpn.* **1989**, *62*, 3012.
(5) Park, J. Ph.D. Thesis, Johns Hopkins University, 1978.
(6) Neuse, E. W.; Loonat, M. S. *Transition Met. Chem.* **1981**, *6*, 260.

0020-1669/92/1331-0177$03.00/0

Chart I

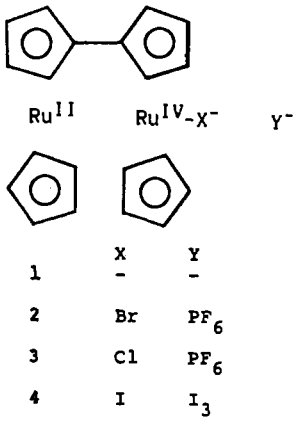

	X	Y
1	-	-
2	Br	PF_6
3	Cl	PF_6
4	I	I_3

hexafluorophosphate salts ($[RcRcX]^+PF_6^-$) (X = Br, **2**; X = Cl, **3**) were generated by the oxidation of **1** with FeX_3 in $HX-NH_4PF_6$ solution.

Solutions of **2** and **3** in acetone or acetonitrile gave deep red-purple solutions different from solutions of $RcHX^+PF_6^-$; the different spectral features suggest the presence of an intramolecular interaction between the Ru^{II} and Ru^{IV} atoms in the mixed-valence species. The present studies were carried out to investigate the chemical state of the two Ru atoms in salts **2** and **3** and in related compounds in the solid state and in solution by means of ^{13}C CP-MAS, ^{13}C NMR, and ^1H NMR spectroscopies.

Experimental Section

Syntheses. Compound **1** was prepared from RcH in high yield (64%) by the following method. RcH (2.0 g, 0.0087 mol) was added to concentrated sulfuric acid (50 mL) at room temperature. The colorless solution changes to deep brown upon heating at ca. 80 °C. After the solution was allowed to stand for 30 min, it was poured into ice water with a large excess of $TiCl_3$ (3.0 g). The deep brown solution changed to colorless. The crude product of **1** was extracted from the solution with benzene (500 mL) and purified by column chromatography (30 mm × 600 mm) on Wako activated alumina (300 mesh). After RcH was eluted by a hexane–benzene (3:1) mixture, **1** was eluted by a hexane–benzene (1:1) mixture. The crude product **1** obtained from the effluent was recrystallized from the hexane–benzene (1:1) mixture as light yellow crystals (1.3 g, 0.0028 mol; yield 64%). Anal. Calcd for $C_{20}H_{18}Ru_2$: C, 52.16; H, 3.94. Found: C, 52.11; H, 3.94. ^1H NMR ($CDCl_3$): δ_H = 4.51 (10 H, s), 4.67 (4 H, t), 4.47 (4 H, t) (lit. ^1H NMR ($CDCl_3$) δ_H = 4.50 (10 H, s), 4.68 (4 H, t), 4.48 (4 H, t)).[6] ^{13}C NMR ($CDCl_3$): δ_C = 70.9 (10 C, s), 71.3 (4 C, s), 69.6 (4 C, s), 87.5 (2 C, s). Infrared spectral data (KBr): 3099.5 m, 1412.0 s, 1382.1 w, 1106.8 s, 1100.5 s, 1062.9 vw, 1028.2 s, 1003.6 s, 875.3 s, 837.7 s, 807.8 s, 445.1 cm^{-1} s.

Compound **3** was prepared by the method similar to that applied for $[RcHCl]^+PF_6^-$.[7] Compound **1** (1.0 g) dissolved in benzene (200 mL) was added to 50 mL of an $FeCl_3$ (4.0 g) solution in 4 M HCl, and the mixture was stirred vigorously for 4 h. The aqueous phase was separated and washed with benzene. By addition of a concentrated NH_4PF_6 solution to the deep brown aqueous solution, the crude salt of **3** was precipitated. The diamagnetic crude product was recrystallized from an acetonitrile–ether mixture as deep red-purple crystals. Anal. Calcd for $C_{20}H_{18}Ru_2ClPF_6$: C, 37.48; H, 2.83. Found: C, 37.22; H, 2.88. Deep red-purple crystals of **2** were obtained similarly to **3** by using $FeBr_3$ and HBr in place of $FeCl_3$ and HCl, respectively. Anal. Calcd for $C_{20}H_{18}Ru_2BrPF_6$: C, 35.05; H, 2.65. Found: C, 35.89; H, 2.92. $[RcRcI]^+I_3^-$ (**4**) and $[BrRc-RcBr]^{2+}(Br_3^-)_2$ (**5**) were prepared by mixing the relevant halogen and the metallocene, respectively, in CCl_4. Anal. Calcd for $C_{20}H_{18}Ru_2I_4$: C, 24.81; H, 1.87. Found: C, 24.88; H, 1.98. Calcd for $C_{20}H_{18}Ru_2Br_8$: C, 21.84; H, 1.65. Found: C, 22.04; H, 1.51. $RcHBr^+PF_6^-$ and $RcHCl^+PF_6^-$ were prepared by the method in the literature.[7]

Physical Methods. ^{13}C CP-MAS NMR spectra were recorded under the conditions similar to those applied in our previous reports.[8-12] The chemical shifts (δ) were compared with adamantane as an external standard and then converted to those from TMS. The assignment of the ^{13}C signals was carried out in comparison with the ^{13}C NMR signals in solution and using dipolar dephasing techniques. Both the ^1H and ^{13}C NMR spectra in solution were recorded on a JEOL FX-200 Fourier transform NMR spectrometer at 199.56 and 50.18 MHz, respectively, using TMS as a standard. An NM-PVT S2 unit (JEOL) was used to control the probe temperatures within a ±0.5 °C accuracy. X-Band ESR spectra of RcH in concentrated sulfuric acid were observed on a JEOL JES-PE-3X ESR spectrometer at room temperature. Electronic absorption spectra were measured in acetonitrile with a Hitachi 220 spctrophotometer at room temperature.

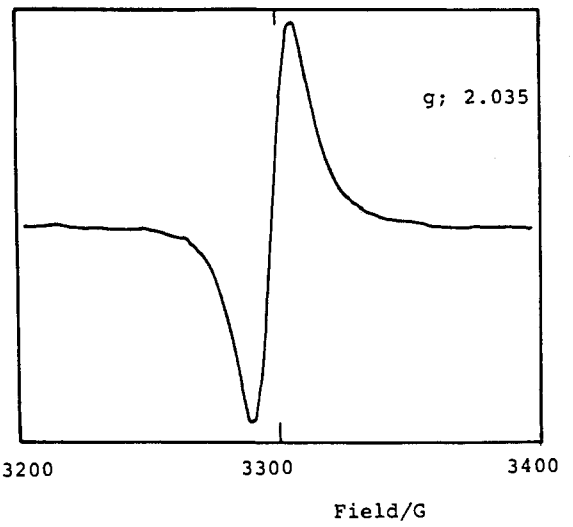

Figure 1. ESR spectrum of RcH in sulfuric acid.

Results and Discussion

Preparation of 1,1″-Biruthenocene (1). The colorless solution of RcH in sulfuric acid gave no ESR signals, but a broad spectrum of g = 2.035, as shown in Figure 1, was observed at room temperature for the brown solution obtained after heating up to 80 °C. This fact suggests the formation of **1** as follows: RcH in sulfuric acid does not give ruthenocenium cation Cp_2Ru^{III} but a ruthenocenyl radical cation, $[Cp(C_5H_4^{\bullet})Ru^{II}]^+$, at once and then the radical cations couple to form a dication $[CpRu(C_5H_4)(C_5H_4)RuCp]^{2+}$ as a precursor of **1** to be reduced with $TiCl_3$. On the other hand, ferrocene and osmocene in the respective sulfuric acid solutions are oxidized at once to ferrocenium and osmocenium cations upon heating up to 80 °C but reduced to the original state again by the addition of $TiCl_3$.

The reason that RcH gives the ruthenocenyl radical upon heating in the sulfuric acid solution differently from ferrocene and osmocene is ascribed to the oxidation potential of Ru in RcH, which is much higher than those of the Fe and Os atoms in ferrocene and osmocene, respectively. The first oxidation potential of Ru has been found to be 0.72 V in acetonitrile, whereas those for the latter two have been found to be 0.44 and 0.50 V, respectively, by our previous results with cyclic voltammetry.[12]

Structures of 2 and 3. Figure 2 shows the ^{13}C CP-MAS NMR spectra of **1** and related compounds. The ^{13}C chemical shift values (δ) are listed in Table I. The Cp-ring carbons show the larger low-field shifts for $RcHX^+PF_6^-$ ($\Delta\delta$ = 22.1 for $RcHBr^+PF_6^-$ and 23.9 for $RcHCl^+PF_6^-$) in comparison with the value for RcH due to Ru–X bond formation.[9,10,12]

In the spectrum of **1** two bands at δ = 87.5 for C_1 and 72.3 for C_5H_5 and $C_{2,5}$ and a shoulder at δ = 69.1 for $C_{3,4}$ are assigned by the selective proton-decoupling technique for ^{13}C NMR in $CDCl_3$.[8] Of the two broad bands observed for **2** (δ = 91.9 and 76.8) and **3** (δ = 92.6 and 76.1), those at the higher frequency

(7) Smith, T. P.; Kwan, K. S.; Taube, H.; Bino, A.; Cohen, S. *Inorg. Chem.* **1984**, *23*, 1943.
(8) Watanabe, M.; Masuda, Y.; Motoyama, I.; Sano, H. *Bull. Chem. Soc. Jpn.* **1988**, *61*, 827.
(9) Watanabe, M.; Masuda, Y.; Motoyama, I.; Sano, H. *Chem. Lett.* **1987**, 1669.
(10) Watanabe, M.; Masuda, Y.; Motoyama, I.; Sano, H. *Chem. Lett.* **1987**, 1981.
(11) Watanabe, M.; Masuda, Y.; Motoyama, I.; Sano, H. *Bull. Chem. Soc. Jpn.* **1988**, *61*, 3479.
(12) Watanabe, M.; Sano, H. *Bull. Chem. Soc. Jpn.* **1990**, *63*, 1455.

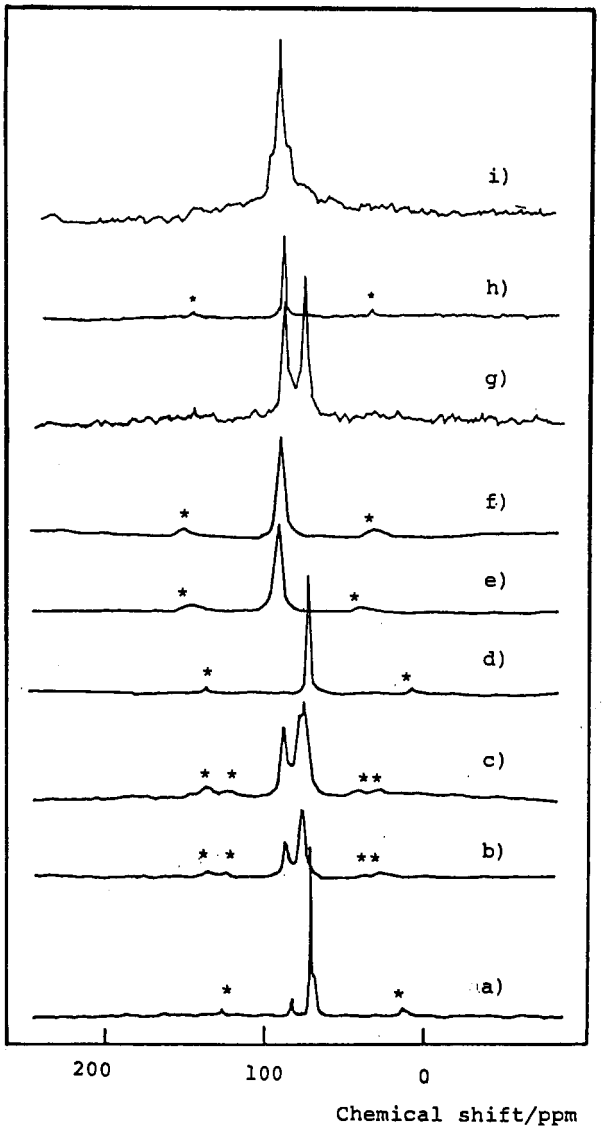

Figure 2. ^{13}C CP–MAS NMR spectra of **1** (a), **2** (b), **3** (c), RcH (d), $RcHBr^+PF_6^-$ (e), $RcHCl^+PF_6^-$ (f), **4** (g), $RcHBr^+Br_3^-$ (h), and **5** (i). Spinning side bands are marked with asterisks.

Table I. ^{13}C Chemical Shifts of Ruthenocene, 1,1″-Biruthenocene (**1**), and Their Salts in the Solid State at Room Temperature

compd	^{13}C chem shift δ/ppm	$\Delta\delta$/ppm
1	87.5 (C_1)	
	72.3 (C_5H_5, $C_{2,5}$)	
	69.1 ($C_{3,4}$)	
2	91.9 (C_5H_4, C_5H_5)	19.6
	76.8 (C_5H_4, C_5H_5)	
	80.6[sh] (C_5H_4)	
3	92.6 (C_5H_4, C_5H_5)	20.3
	76.1 (C_5H_4, C_5H_5)	
	80.2[sh] (C_5H_4)	
4	92.9 (C_5H_4, C_5H_5)	20.6
	77.4 (C_5H_4, C_5H_5)	
	114.6 (C_1)	
	94.7 (C_1)	
5	96.4 (C_5H_4, C_5H_5)	24.1
RcH	73.2 (C_5H_5)	
$RcHBr^+PF_6^-$	95.3 (C_5H_5)	22.1
$RcHCl^+PF_6^-$	97.1 (C_5H_5)	23.9
$RcHBr^+Br_3^-$	96.9 (C_5H_5)	23.7
$RcHI^+I_3^-$	93.4 (C_5H_5)	21.1

side are assigned to C_5H_5 and $C_{2,3,4,5}$ as in the case of **1**. Those at the lower frequency side were unable to be assigned to C_1 similarly, since the band assigned to the $RcHX^+$ moiety in

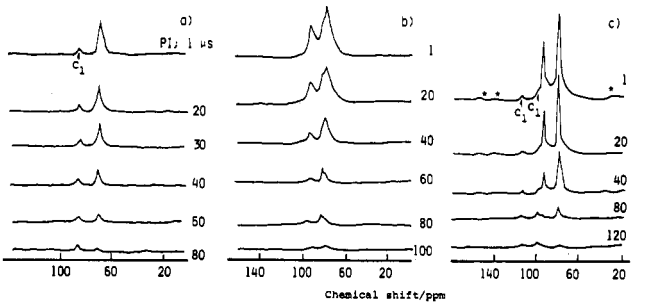

Figure 3. Dipolar dephasing ^{13}C CP–MAS NMR spectra of **1** (a), **2** (b), and **4** (c).

Table II. ^1H Chemical Shifts of Ruthenocene, 1,1″-Biruthenocene (**1**), and Their Salts in Acetone, Acetonitrile, and Nitromethane Solution at the Indicated Temperatures

compd	temp/K	^1H chem shift δ_H/ppm	$\Delta\delta_H$/ppm
1	298	4.68, 4.44 ($H_{2,5}$, $H_{3,4}$)	
		4.48 (C_5H_5)	
	183	4.69, 4.43 ($H_{2,5}$, $H_{3,4}$)	
		4.46 (C_5H_5)	
2	323	5.81, 5.48 ($H_{2,5}$, $H_{3,4}$)	
		5.35 (C_5H_5)	0.88
	183	6.38, 5.71 ($H_{2,5}$, $H_{3,4}$)	
		6.00 (C_5H_5)	1.54
		5.32 ($H_{2,5}$, $H_{3,4}$)	
		4.75 (C_5H_5)	0.29
3	298	5.76, 5.40 ($H_{2,5}$, $H_{3,4}$)	
		5.30 (C_5H_5)	0.83
	183	6.31, 5.73 ($H_{2,5}$, $H_{3,4}$)	
		5.94 (C_5H_5)	1.48
		5.30, 5.27 ($H_{2,5}$, $H_{3,4}$)	
		4.75 (C_5H_5)	0.29
4	333	5.72, 5.64 ($H_{2,5}$, $H_{3,4}$)	
		5.30 (C_5H_5)	0.83
	183	6.41, 5.76 ($H_{2,5}$, $H_{3,4}$)	
		6.05 (C_5H_5)	1.59
		5.33, 5.19 ($H_{2,5}$, $H_{3,4}$)	
		4.61 (C_5H_5)	0.15
RcH	298	4.51 (C_5H_5)	
	183	4.51 (C_5H_5)	
$RcHBr^+PF_6^-$	298	6.29 (C_5H_5)	1.78
	183	6.34 (C_5H_5)	1.83
$RcHCl^+PF_6^-$	298	6.25 (C_5H_5)	1.74
	183	6.29 (C_5H_5)	1.78
$RcHI^+I_3^-$	298	6.38 (C_5H_5)	1.87
	183	6.43 (C_5H_5)	1.92
RcH[a]	298	4.53 (C_5H_5)	
$RcHBr^+PF_6^-$[a]	298	5.95 (C_5H_5)	1.42
$RcHCl^+PF_6^-$[a]	298	5.95 (C_5H_5)	1.42
$RcHI^+I_3^-$[a]	298	6.10 (C_5H_5)	1.57
1[a]	298	4.69, 4.46 ($H_{2,5}$, $H_{3,4}$)	
		4.46 (C_5H_5)	
2[a]	298	5.61, 5.12 ($H_{2,5}$, $H_{3,4}$)	
		5.20 (C_5H_5)	0.741
3[a]	298	5.59, 5.12 ($H_{2,5}$, $H_{3,4}$)	
		5.18 (C_5H_5)	0.72
5[b]	273	6.45, 6.10 ($H_{2,5}$, $H_{3,4}$)	
		6.19 (C_5H_5)	
$RcHBr^+PF_6^-$[b]	273	6.11 (C_5H_5)	
4[b]	353	5.68, 5.49 ($H_{2,5}$, $H_{3,4}$)	
		6.28 (C_5H_5)	

[a] In acetonitrile. [b] In nitromethane.

$RcHX^+PF_6^-$ was observed at δ = 97.1 for X = Cl and at δ = 95.3 for X = Br. The dipolar dephasing technique proposed by Munowitz et al.[13] was applied to ascertain the assignment. By the increasing of the proton–carbon nondecoupling time (PI), the band at the lower frequency side decayed slowly for **1** to support the

(13) Monowitz, M. G.; Griffin, R. G.; Bodenhausen, G.; Huang, T. H. *J. Am. Chem. Soc.* **1981**, *103*, 2529.

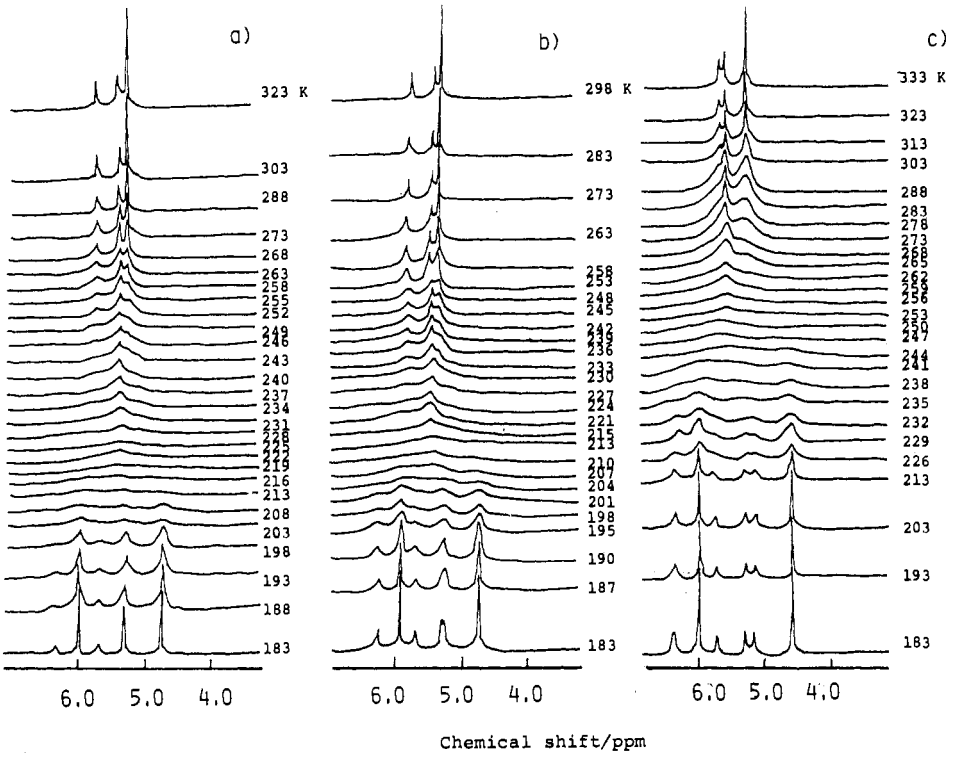

Figure 4. Temperature-dependent ^1H NMR spectra of **2** (a), **3** (b), and **4** (c) in acetone at indicated temperatures.

assignment to C_1 (Figure 3a). However, those for **2** (as shown in Figure 3b) and **3** decayed rapidly as well as the bands at the higher frequency side. Hence, the bands at the lower side were assigned to the Cp-ring carbons of the $[Cp(C_5H_4)RuX]^+$ moiety and those at the higher side to the ruthenocenyl group $RuCp(C_5H_4)$. Accordingly a formula $[Ru^{II}Cp(C_5H_4)(C_5H_4)Ru^{IV}X]^+PF_6^-$ can be given to **2** and **3**.

In **2** and **3**, the chemical shift in the $Cp(C_5H_4)Ru$ moiety increases slightly (3–5 ppm) and that in $[Cp(C_5H_4)RuX]^+$ decreases slightly (3–5 ppm) in comparison with those in **1**, RcH, and $RcHX^+PF_6^-$. The variation can be interpreted in terms of an intramolecular interaction between both the moieties through the 1,1′-bis(2,4-cyclopentadienylidene) group, $(C_5H_4)(C_5H_4)$, in **2** and **3**. As has been mentioned in the Introduction, deep purple acetone solutions of **2** and **3** are quite different in color and other spectral features from solutions of $RcHX^+PF_6^-$.

Temperature dependencies of the ^1H NMR spectra in acetone solutions support the presence of the intramolecular interaction between Ru^{II} and Ru^{IV} through $(C_5H_4)(C_5H_4)$ in **2** and **3**. As shown in Figure 4a,b, the spectra of **2** and **3** exhibit remarkable changes depending on temperature, whereas those of **1**, RcH, and $RcHX^+PF_6^-$ are independent to temperature. Among the three sharp bands, δ_H = 5.81 (4 H), 5.48 (4 H), and 5.35 ppm (10 H), observed for **2** at 323 K, the strong peak of 5.35 ppm has a value close to the average of the bands at 4.48 ppm for **1** and 6.29 ppm for $RcHBr^+PF_6^-$, respectively, assigned to the Cp-ring protons. Upon cooling, the three peaks are broadened and the coalescence temperature (T_c) for the main Cp-ring signals is found to be ca. 228 K. At 183 K new bands become distinguishable at δ = 6.38 (2 H), 6.00 (5 H), 5.71 (2 H), 5.32 (4 H), and 4.75 ppm (5 H); the 6.00 (5 H) and 4.75 ppm (5 H) peaks are assigned to the Cp-ring protons of $[Cp(C_5H_4)Ru^{IV}Br]^+$ and $Cp(C_5H_4)Ru^{II}$, respectively. Hence, **2** is concluded to take on the trapped-valence state $[Ru^{II}Cp(C_5H_4)(C_5H_4)CpRu^{IV}Br]^+PF_6^-$ in acetone at 183 K as well as in the solid state. However, the respective chemical shifts increased by 0.29 ppm for the $Cp(C_5H_4)Ru^{II}$ moiety compared to that for **1** and decreased by 0.34 ppm for the $Cp(C_5H_4)Ru^{IV}Br^+$ moiety compared to that for $RcHBr^+PF_6^-$, which suggests an intramolecular interaction between both moieties still remains to a certain extent at 183 K.

The lifetime, τ, of the electron transfer between Ru^{II} and Ru^{IV} for **2** was estimated to be 1.81×10^{-3} s at T_c = 228 K from the equation $\tau = 2^{1/2}\pi^{-1}\delta_\nu^{-1}$,[14] where δ_ν in hertz is the difference in the chemical shift between the main peak for the Cp ring of the ruthenocenyl group and that for $[Cp(C_5H_4)Ru^{IV}Br]^+$ (249.45 Hz for 1.25 ppm). The value of the activation energy at T_c, $\Delta G^*(T_c)$, was given as 43.4 kJ mol^{-1} from the equation $\Delta G^*(T_c) = 2.303RT_c(10.319 + \log \tau + \log T_c)$, where R is the gas constant.[15]

Results similar to those for **2** were obtained for **3**. As shown in Figure 4b, the similar spectral features gave slightly smaller values of δ_ν = 237.48 Hz and T_c = 213 K and a greater value of $\tau = 1.90 \times 10^{-3}$ s; $\Delta G^*(T_c)$ = 40.5 kJ mol^{-1} was also a little smaller than that for **2**. In acetonitrile solutions, the temperature dependency of the ^1H NMR spectrum between 229 and 333 K has been observed as similar to those in acetone for **2** and **3**.

The ^{13}C NMR spectrum in acetone solution also supports intramolecular electron transfer between the Ru^{II} and Ru^{IV} for **2** and **3**. The temperature-dependent spectra are shown in Figure 5a,b; the δ_C values are listed in Table III. In comparison with the data for RcH and $RcHBr^+PF_6^-$, and those obtained from the above mentioned solid-state ^{13}C NMR spectrum, the sharp and strong peaks at 90.72 and 75.54 ppm were assigned to the Cp-ring carbon atoms of the $[Cp(C_5H_4)Ru^{IV}Br]^+$ and $[Cp(C_5H_4)Ru^{II}]$ moieties, respectively, for **2** at 183 K. Although the C_1 bands for both the moieties were too weak to be detected, the observation at 183 K also supports the trapped-valence state of **2**.

Upon heating of the sample to 243 K, the peaks become broadened; T_c for the main Cp-ring signals is given as ca. 243 K. Above the T_c, three sharp bands appear at 84.01 (10 C), 83.57 (4 C), and 77.25 ppm (4 C) at 313 K for **2**. The value of 84.01 ppm is very close to the average, 83.13 ppm, between the value for $[Cp(C_5H_4)Ru^{IV}Br]^+$ (90.72 ppm) and $[Cp(C_5H_4)Ru^{II}]$ (75.54 ppm). The values of $\tau(T_c) = 5.91 \times 10^{-4}$ s and $\Delta G^*(T_c)$ = 44.1 kJ mol^{-1} have been obtained.

Similarly, the values of T_c = 223 K, $\tau(T_c) = 5.47 \times 10^{-4}$ s, and $\Delta G^*(T_c)$ = 40.2 kJ mol^{-1} were obtained for **3**. The values of δ_ν defined for ^{13}C similarly to ^1H at 183 K, and of δ_C of the main peak at 313 K, are respectively greater by 1.21 and 0.10 ppm for **3** than for **2**. This suggests the Ru^{IV}–Br bond is less stable than the Ru^{IV}–Cl bond in acetone. Actually **2** is gradually reduced

(14) Gutowsky, H. S.; Holm, C. H. *J. Chem. Phys.* **1956**, *25*, 1228.
(15) Glastone, S.; Laidler, K. J.; Eyring, H. *The Theory of Rate Process*; McGraw-Hill Book Co., Inc.: London, 1941, Chapter 1.

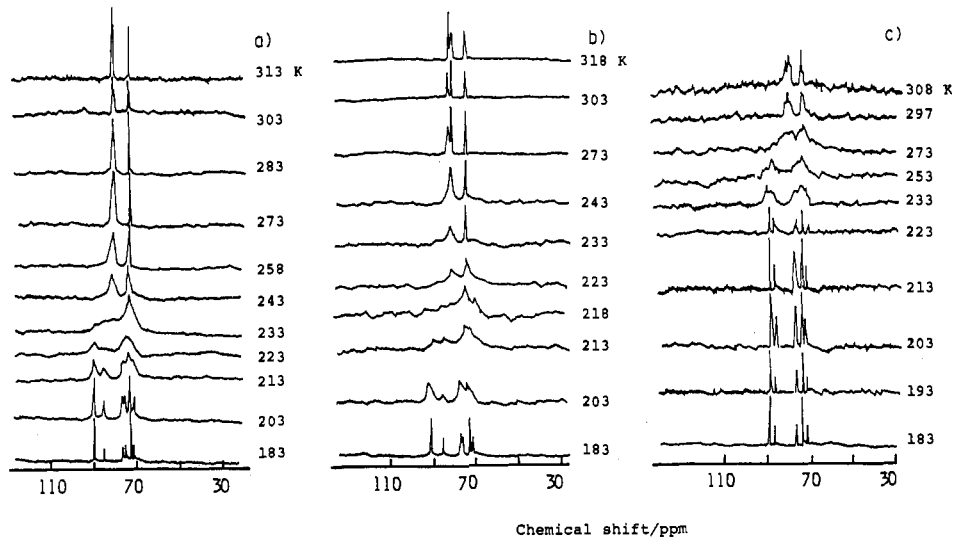

Figure 5. Temperature-dependent ^{13}C NMR spectra of **2** (a), **3** (b), and **4** (c) in acetone at indicated temperatures.

Table III. ^{13}C Chemical Shifts of 1,1″-Biruthenocene (**1**), Ruthenocene, and Their Salts in Acetone

compd	temp/K	^{13}C chem shift δ_C/ppm
1	298	72.09 ($C_{2,5}$)
		71.31 (C_5H_5)
		68.35 ($C_{3,4}$)
2	313	84.01 (C_5H_5)
		83.57, 77.25 ($C_{2,5}$, $C_{3,4}$)
	183	90.72 (C_5H_5)
		86.63, 77.39 ($C_{2,5}$, $C_{3,4}$)
		75.54 (C_5H_5)
		78.56, 73.69 ($C_{2,5}$, $C_{3,4}$)
3	318	84.11 (C_5H_5)
		83.09, 77.25 ($C_{2,5}$, $C_{3,4}$)
	183	91.94 (C_5H_5)
		86.45, 78.23 ($C_{2,5}$, $C_{3,4}$)
		75.55 (C_5H_5)
		78.91, 73.99 ($C_{2,5}$, $C_{3,4}$)
4	308	83.58 (C_5H_5)
		82.41, 76.28 ($C_{2,5}$, $C_{3,4}$)
	183	88.64 (C_5H_5)
		86.50, 77.01 ($C_{2,5}$, $C_{3,4}$)
		74.87 (C_5H_5)
		77.45, 72.92 ($C_{2,5}$, $C_{3,4}$)
RcH	298	70.50 (C_5H_5)
	228	70.54 (C_5H_5)
	183	70.63 (C_5H_5)
$RcHCl^+PF_6^-$	298	96.76 (C_5H_5)
	223	96.40 (C_5H_5)
	183	96.27 (C_5H_5)
$RcHBr^+PF_6^-$	298	95.06 (C_5H_5)
	228	64.82 (C_5H_5)
	183	94.67 (C_5H_5)
$RcHI^+I_3^-$	223	91.46 (C_5H_5)
	203	91.46 (C_5H_5)
	183	91.41 (C_5H_5)

in acetone at temperatures above 313 K, whereas **3** is stable under the same conditions.

These NMR spectroscopic observations indicate there occurs a rapid intramolecular electron transfer between Ru^{II} and Ru^{IV} in the Rc–RcX^+ species with the exchange of X at higher temperatures, $[Ru^{II}Cp(C_5H_4)Cp(C_5H_4)Ru^{IV}X]^+ \rightleftharpoons [XRu^{IV}Cp(C_5H_4)Cp(C_5H_4)Ru^{II}]^+$, in acetone and acetonitrile. The averaged-valence state, in the NMR time scale, can also be described as a μ-halo structure of $[Cp(C_5H_4)Ru^{III}\cdots X\cdots Ru^{III}(C_5H_4)Cp]^+$.

The electronic absorption spectra at room temperature support this conclusion. Figure 6 shows the electronic absorption spectra of $RcHBr^+PF_6^-$ (a), **2** (b), **3** (c), and **4** (d) in acetonitrile, which was used as the solvent because the salts are more stable than in acetone. The strong absorption band at 395 nm (ϵ 1120) for the $RcHBr^+PF_6^-$ solution, assigned to $RcHBr^+$,[16] blue shifts by 50–55

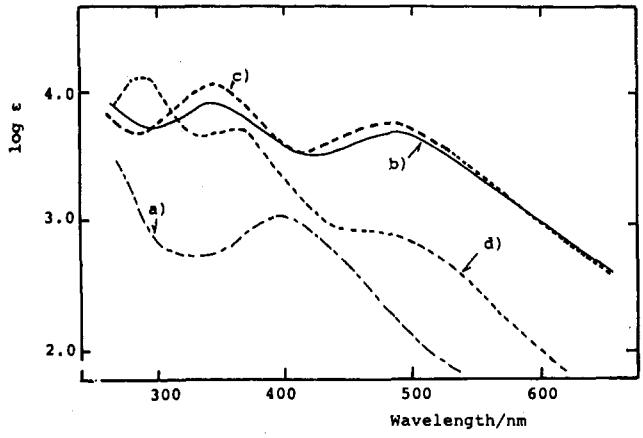

Figure 6. Electronic absorption spectra of $RcHBr^+PF_6^-$ (a), **2** (b), **3** (c), and **4** (d) compounds in acetonitrile.

nm in the solutions of **2** (335 nm, ϵ 8920) and **3** (340 nm, ϵ 12590). New bands appear at 480 nm (ϵ 5600) and 470 nm (ϵ 7080) for **2** and **3**, respectively, while no corresponding bands are observed for RcH, **1**, and $RcHX^+PF_6^-$. Although the intervalence electron-transfer band is observed in the infrared region for mixed-valence binuclear ferrocene derivatives,[1,2] the bands at 480 and 470 nm may be assigned to the intramolecular electron transfer between Ru^{II} and Ru^{IV} in **2** and **3**, respectively.

Structures of 4 and 5. Dark brown compounds $RcRcI_4$ (**4**) and $RcRcBr_8$ (**5**) are obtained by the reaction of **1** with elemental halogens I_2 and Br_2 in an organic solvent such as carbon tetrachloride, benzene, hexane, ether, etc. As for **4** and **5**, the ^{13}C CP-MAS NMR spectra have already been included in Figure 2; Figures 3–6 also contain the respective spectra for **4**.

In the ^{13}C CP-MAS NMR spectrum, the broad single band of **5** at δ_C = 96.4 ppm coincides with that observed for $[RcHBr]^+Br_3^-$ at 96.9 ppm, as shown in Figure 2i,h).[7] Hence the formula $[BrRu^{IV}Cp(C_5H_4)(C_5H_4)CpRu^{IV}Br]^{2+}(Br_3^-)_2$ is given to **5**.

On the other hand, **4** gives two broad bands at 92.9 and 77.4 ppm. In the dipolar dephasing observations, both the two main peaks decay similarly depending on the PI time (Figure 3c). In comparison with the δ_C values of $RcHI^+I_3^-$ (93.4 ppm) and **1** (72.3 ppm), the 92.9 ppm peak is assigned to the Cp-ring carbons of $[Cp(C_5H_4)RuI]^+$ and the 77.4 ppm peak to those of the ruthe-

(16) Borrel, D.; Henderson, E. *J. Chem. Soc., Dalton Trans.* **1975**, 433.
(17) Sohn, Y. S.; Schlueter, A. W.; Hendrickson, D. N.; Gray, H. B. *Inorg. Chem.* **1974**, *13*, 301.
(18) Morrison, W. H., Jr.; Hendrickson, D. N. *Chem. Phys. Lett.* **1973**, *22*, 119.

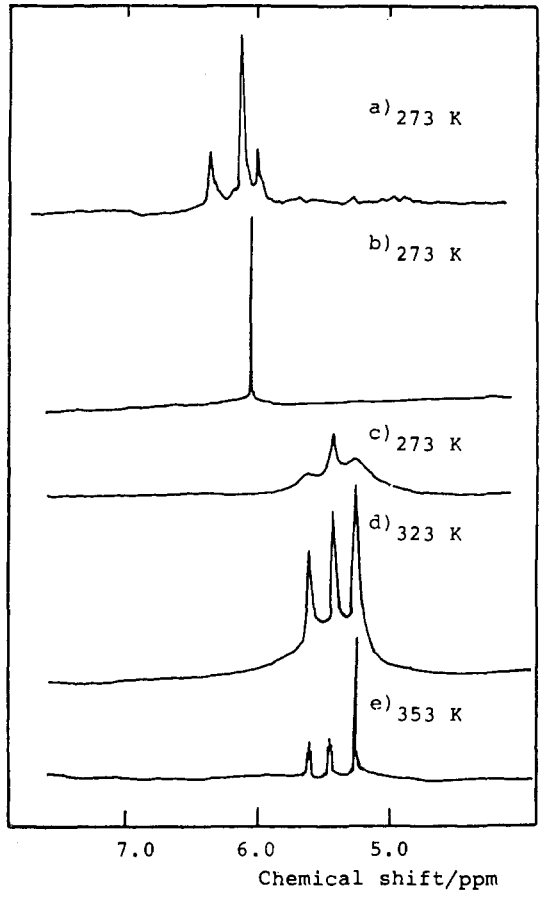

Figure 7. ^{1}H NMR spectra of **5** (a), $RcHBr^+PF_6^-$ (b), and **4** (c–e) salts in nitromethane at indicated temperatures.

nocenyl group. The two weak bands at 114.6 and 94.7 ppm decay slowly, remaining even after so long a PI time of 120 μs that the main peaks collapsed. The former is assigned to the C_1 carbon of $[Cp(C_5H_4)RuI]^+$, and the latter, to that of the ruthenocenyl group. Hence, the formulation $[Ru^{II}Cp(C_5H_4)(C_5H_4)CpRu^{IV}I]^+I_3^-$ is given to **4**. The reason that **1** is oxidized to the dicationic salt, **5**, by Br_2 but to the monocationic one, **4**, by I_2 is due to the higher oxidation potential of Br_2 compared to I_2.

The dicationic salt, **5**, is very soluble in acetone and acetonitrile, giving a yellow-green solution, which is so unstable at room temperature that the color changes to deep red within a few minutes; it is a little more stable in nitromethane at 273 K. Figure 7 shows the ^{1}H NMR spectra of **5** (a) and monocationic salts $RcHBr^+PF_6^-$ (b) and **4** (c–e) in nitromethane at the indicated temperatures. Among the three peaks observed for **5** at 6.45 (4 H), 6.10 (4 H), and 6.19 ppm (10 H), the main peak at 6.19 ppm is very close to that at 6.11 ppm observed for $RcHBr^+PF_6^-$; **4** gives the peaks at 5.68 (4 H), 5.49 (4 H), and 6.28 ppm (10 H) at 353 K. Hence **5** retains the state of $[BrRu^{IV}Cp(C_5H_4)(C_5H_4)CpRu^{IV}Br]^{2+}(Br_3^-)_2$ in nitromethane solution at 273 K.

Compound **4** is more stable than **5** in acetone, acetonitrile, and nitromethane. Figure 4c shows the temperature dependency of the ^{1}H NMR spectrum in acetone. Among the bands observed at 333 K, the main peak at 5.30 ppm (10 H) is assigned to the Cp-ring protons in the $Cp(C_5H_4)Ru$ and $[Cp(C_5H_4)RuI]^+$ moieties. Upon cooling of the sample to 253 K, the peaks are almost flattened; T_c = 253 K is by ca. 25–40° higher than those of **2** and **3**. At 183 K the peaks are observed assignable to the Cp-ring protons of $[(C_5H_4)CpRuI]^+$ at 6.05 ppm and to those in the ruthenocenyl group at 4.61 ppm as is the case for **2** and **3**. The results are consistent with the formula $[Ru^{II}Cp(C_5H_4)(C_5H_4)CpRu^{IV}I]^+I_3^-$ at 183 K. The value of $\tau = 1.56 \times 10^{-3}$ s and $\Delta G^*(T_c)$ = 48.0 kJ mol^{-1} have been obtained. The ^{1}H NMR spectra of **4** in nitromethane (Figure 7c–e) and in acetonitrile also show temperature dependencies similar to those in acetone. The electron transfer may be slower in **4** than in **2** and **3** because of the higher T_c and the greater $\Delta G^*(T_c)$ values.

The temperature-dependent ^{13}C NMR spectrum of **4** in acetone also shows features similar to those for **2** and **3** (Figure 5c). The values of T_c = 273 K, $\tau(T_c) = 6.51 \times 10^{-4}$ s, and $\Delta G^*(T_c)$ = 50.0 kJ mol^{-1} were obtained. The spectra at temperatures higher than T_c are not so sharp as those found for **2** and **3** probably due to the instability of **4** in acetone; relatively broad bands were observed at 83.58 (10 C), 82.41 (4 C), and 76.28 ppm (4 C) at 308 K.

In the electronic absorption spectrum of **4** in acetonitrile at room temperature (Figure 6d), a new band was observed at 480 nm along with the bands at 290 and 360 nm assigned to I_3^- in comparison with that of $RcHBr^+PF_6^-$.

From these observations we concluded that there occurs an intramolecular electron transfer between the Ru^{II} and Ru^{IV} atoms in the mixed-valence states of **2**–**4** in acetone and other organic solvents associated with the exchange reaction of the halogen atom: $[Ru^{II}*Cp(C_5H_4)(C_5H_4)CpRu^{IV}X]^+ \rightleftharpoons [XRu^{IV}*Cp(C_5H_4)(C_5H_4)CpRu^{II}]^+$ (X = Cl, Br, I). The rate of electron transfer increases in the order **4** < **2** < **3** and gradually decreases by a lowering of temperature to give a coalescence temperature T_c, under which the biruthenocenium species takes on the trapped-valence state $[Ru^{II}Cp(C_5H_4)(C_5H_4)CpRu^{IV}X]^+Y^-$ similar to the valence state found in the solid structure at room temperature.

Registry No. **1**, 67126-04-9; **2**, 137916-60-0; **3**, 137916-62-2; **4**, 137916-64-4; **5**, 137916-66-6; RcH, 1287-13-4; $RcHBr^+PF_6^-$, 90109-04-9; $RcHCl^+PF_6^-$, 90109-03-8; $RcHBr^+Br_3^-$, 39427-30-0; $RcHI^+I_3^-$, 39427-31-1.